Available online at www.sciencedirect.com

ScienceDirect

Physics Procedia 76 (2015) 160 – 164

Physics Procedia

The 17th International Conference on Luminescence and Optical Spectroscopy of Condensed Matter (ICL2014)

Enhanced Near-Infrared Upconversion Emission of Yb^{3+}-Tm^{3+} co-doped Gd_2O_3 Sub-microrods

D.K. Xu[a], C.F. Liu[a], J.W. Yan[a], H.Q. Ouyang[a], S.H. Yang[a], Y.L. Zhang[a,*]

[a]*State Key Laboratory of Optoelectronic Materials and Technologies, Sun Yat-sen University, No.135 Rd. Xingangxi, Haizhu District, Guangzhou 510275, PR China*

Abstract

Lanthanide-doped rare-earth oxides have aroused great interest in display and bio-probe technology due to their excellent luminescent and magnetic performance. In this paper, Gd_2O_3 sub-microrods (SMRs) with cubic structure are obtained via heat-treatment from gadolinium hydroxides precursor. Upconversion (UC) spectra show intense near-infrared (NIR) emission which is assigned to $^3H_4 \rightarrow {}^3H_6$ transition of Tm^{3+}. From the double logarithmic plot of emission intensity versus pump powers, it was seen that typical two photons were involved in the NIR UC process. Moreover, a series of Gd_2O_3:18%Yb^{3+},x%Tm^{3+} (x = 0.1, 0.5, 1, 2, 5) and Gd_2O_3:y%Yb^{3+},0.5%Tm^{3+} (y = 1, 5, 10, 40, 80) SMRs were prepared and characterized to explore their NIR emission properties. Finally, the enhanced NIR emission property was found in Gd_2O_3:Yb^{3+},Tm^{3+} SMRs from the reduced NaOH concentration and the reduced calcinations temperatures.

Peer-review under responsibility of The Organizing Committee of the 17th International Conference on Luminescence and Optical Spectroscopy of Condensed Matter

Keywords: Gd_2O_3; sub-microrods; upconversion; enhanced NIR emission

1. Introduction

Recently, lanthanide-doped upconversion (UC) luminescent materials have aroused great attention due to their wide potential applications in optoelectronic devices (Johnson et al. (2002)), panel display (Wang et al. (1998)),

* Corresponding author. Tel.: +020-84113903; fax: +020-84113397.
E-mail address: stszyl@mail.sysu.edu.cn

Peer-review under responsibility of The Organizing Committee of the 17th International Conference on Luminescence and Optical Spectroscopy of Condensed Matter
doi:10.1016/j.phpro.2015.10.029

biolabeling (Bruchez et al. (1998)) and photovoltaic (Law et al. (2005)). Among them, rare-earth sesquioxides are ideal host matrixes because of their good chemical stability and low phonon energy (~ 600 cm^{-1}), especially Gd_2O_3, which can be considered the most perspective one for the intrinsic magnetic and luminescent properties. The UC process, especially the two-photon involved red emission and even near-infrared (NIR) emission, is suitable for in vivo bioimaging due to the minimal photo damage to living organisms, weak background fluorescence, high sensitivity and high penetration depth in tissues (Wang and Li (2007), Zhang et al. (2007)). Yb^{3+}-Tm^{3+} codopants systems have been studied recently for their high efficiency NIR luminescence. For example, Chen et al. (2010) reported the enhanced NIR emission of $NaYF_4$:Yb^{3+},Tm^{3+} nanocrystals with smaller size. Chang et al. (2013) found a strong NIR emission in $NaYF_4$:Yb^{3+},Tm^{3+}/QDs nanoheterostructures. Liu et al. (2014) prepared $NaYF_4$:Yb^{3+},Tm^{3+} microcrystals the controllable morphology and found the enhanced NIR emission with decreased pH values of initial solutions. Herein, we report the enhanced NIR emission in Gd_2O_3:Yb^{3+},Tm^{3+} system, with controllable morphology of the precursor $Gd(OH)_3$ either through modulating alkaline base concentration or calcination temperatures.

2. Experimental Details

All materials were used without further purification. Gd_2O_3:Yb^{3+},Tm^{3+} sub-microrods (SMRs) were prepared as following: Total amount of 1 mmol $Ln(NO_3)_3$ in 10 mL deionized water was mixed with EDTA alkaline solution. After 30 min vigorous agitation, the resultant suspension was poured into a 50 mL Teflon and mixed with DI water until the volume of suspension was about 60% of the Teflon. Finally the Teflon was sealed into the autoclave and heated at 200 ℃ for 12 h. The final products were collected with precipitation and washed with ethanol twice and annealed at 700 ℃ for 2 h in a furnace.

Samples derived from different NaOH concentration were prepared with the same procedure, except that EDTA was dissolved into alkaline solution that contains different NaOH concentration. Samples undergone different annealing temperatures were also prepared by adjusting the furnace temperature to 700 ℃, 900 ℃ and 1100 ℃, respectively.

Phase structure and morphology of the as-prepared samples were characterized on a Rigaku Company D-Max 2200VPC X-ray diffraction (XRD) (Cu $K_{\alpha 1}$ radiation, λ = 1.54056Å) and JEOL JSM 6060 scanning electronic microscopy (SEM) (V = 20 kV, working distance = 15 mm), respectively. Photoluminescence spectra were performed on Edinburgh Instrument Company FLS920 Combined Fluorescence Life and Steady-State Fluorescence Spectrometer equipped with a 2 W 980 nm (spot area is about 0.05 cm^2) continuous laser diode.

3. Results & Discussion

3.1. Structure

Phase structures of the precursor $Gd(OH)_3$ and Gd_2O_3 are identified via XRD, shown in Fig. 1(a), as the typical hexagonal (space group P-6) and cubic phase (space group Ia-3), respectivly, without any other purity phases according to the standard JCPDS data presented as vertical lines. The morphologies of $Gd(OH)_3$ and Gd_2O_3 system are shown in Fig. 1(b) and (c). The SEM image in Fig. 1(b) shows that $Gd(OH)_3$ sample consists of uniform SMRs in high yield with diameter about 0.8 μm and length about 2.2 μm. One can observe that the SMRs are straight and the surfaces are smooth. It can also be seen that the ends of these SMRs are rather tough from the inset of Fig. 1(b). After the heat-treatment, Gd_2O_3 samples can be obtained. From Fig. 1(c), one can see that the calcined sample is composed of similar rod-like microcrystals in high yield, inheriting their parents' morphology. These SMRs also have rough ends and are also straight. However, rough surfaces also occur to the SMRs, which is probably due to the loss of H_2O and is of high crystallinity under high calcination temperature.

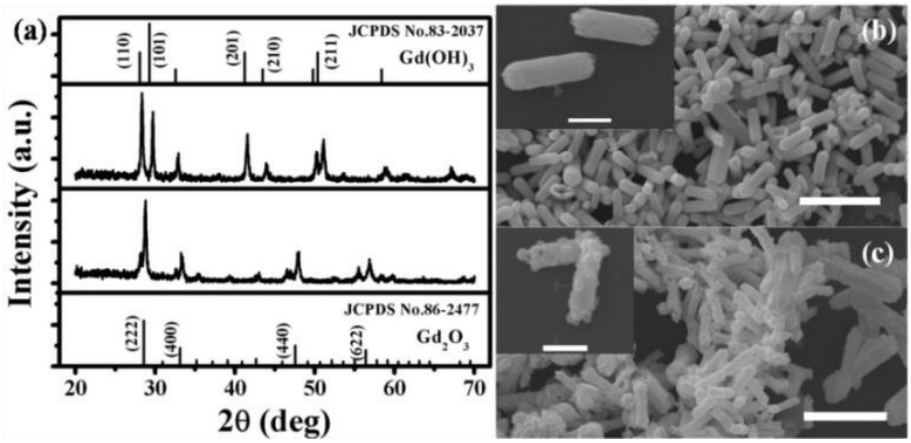

Fig. 1 (a) XRD pattern of $Gd(OH)_3$ and Gd_2O_3 samples and SEM images of (b) $Gd(OH)_3$ and (c) Gd_2O_3 samples, respectively. (Scale bar = 5 μm) Insets show the high magnification images of $Gd(OH)_3$ and Gd_2O_3. (Scale bar = 1μm)

3.2. Upconversion Luminescence Property

Fig. 2 reveals the UC luminescence of Gd_2O_3:18%Yb^{3+},0.5%Tm^{3+} SMRs under 980 nm excitation. The intense NIR emission around 800 nm is observed, which is assigned to Tm^{3+} $^3H_4 \rightarrow {}^3H_6$ transition. The visible emissions, including Tm^{3+} $^1G_4 \rightarrow {}^3H_6$ (blue emission) and $^1G_4 \rightarrow {}^3F_4$ (red emission) transitions, can hardly be observed. To explore the UC mechanism, a double logarithmic relationship between NIR emission intensity and pump powers is established, which can be seen from the inset of emission spectra. The slope is about 2.4, indicating that two photons are involved in the UC process. The UC process is briefly described in the illustration of energy transfer between Yb^{3+} and Tm^{3+}. Two pathways, $^3H_6 \rightarrow {}^3H_5$ and $^3F_4 \rightarrow {}^3F_{2,3}$ transitions, occur in the UC process, which is due to the UC energy transfer between Yb^{3+} and Tm^{3+}. When the electronic energy is relaxed to $^3H_4$ manifolds through phonons, the NIR emission takes place due to electrons in $^3H_4$ excited state transferring back to $^3H_6$ ground state.

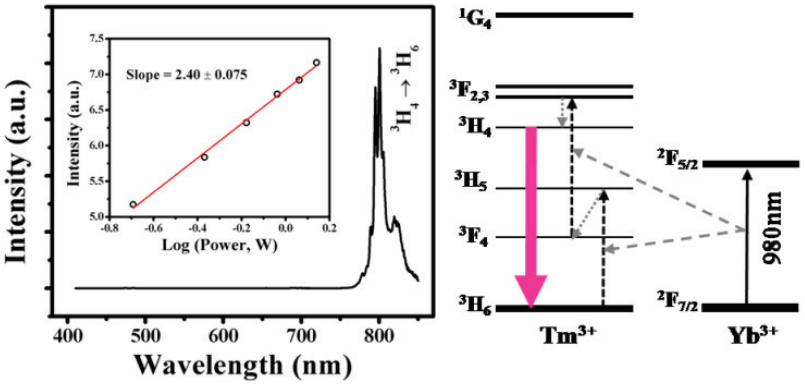

Fig.2 (Left) UC emission spectra of Gd_2O_3:18%Yb^{3+},0.5%Tm^{3+} SMRs under 980 nm excitation. Inset shows the double logarithmic relationship between intensity and power. (Right) Illustration of energy transfer between Yb^{3+} and Tm^{3+}.

In order to study the concentration-dependent UC luminescence, different dopant concentrations are used in Gd_2O_3 SMRs. Fig. 3 shows the emission spectra of Gd_2O_3:Yb^{3+},Tm^{3+} SMRs doped with different Tm^{3+} and Yb^{3+} concentration, respectively. Intense NIR emission is well observed while the visible emissions can hardly be seen. From Fig. 3(a), 0.5%Tm^{3+} doped Gd_2O_3:18%Yb^{3+} SMRs show strongest NIR emission. When the concentration of Tm^{3+} is greater than 0.5%, the NIR emission largely decreased due to heavy concentration that would eliminate the emission through relaxation, which is the so called concentration quenching. Additional, different sensitizer Yb^{3+}

concentration doped Gd_2O_3:0.5%Tm^{3+} SMRs were also prepared. From the emission spectra in Fig. 3(b), one can observe that 18%Yb^{3+},0.5%Tm^{3+} codoped Gd_2O_3 SMRs also show the strongest emission intensity compared to other Yb^{3+} concentrations. When Yb^{3+} concentration is over 18%, the NIR emission intensity severely reduces due to closer Yb^{3+}-Tm^{3+} distance that would lead to relaxation and thus eliminate the luminescence. From the above results, the optimal Yb^{3+} and Tm^{3+} concentrations are 18% and 0.5%, respectively, which is similar to Mahalingam et al(2009) under low power density.

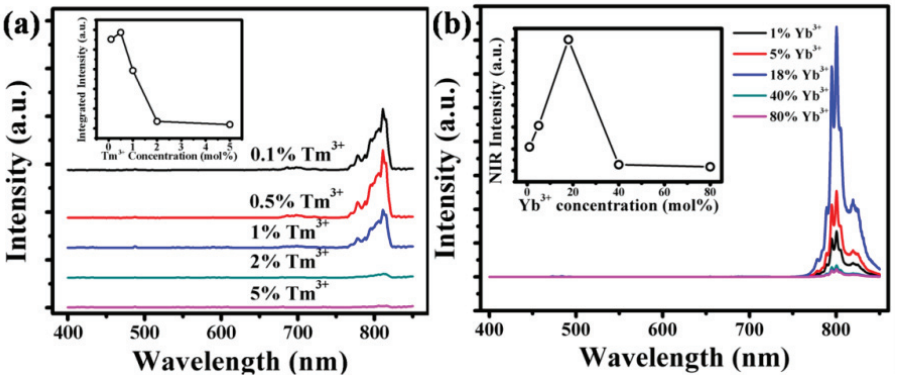

Fig.3 UC emission spectra of (a) different Tm^{3+} concentration doped Gd_2O_3:18%Yb^{3+} and (b) different Yb^{3+} concentration doped Gd_2O_3:0.5%Tm^{3+} SMRs, respectively. Insets are relationship between integrated intensity and different dopant concentrations. The power density of the laser is about 14.1 W/cm^2.

3.3. Enhanced NIR Emission

Sodium hydroxide plays an important role in the formation and crystal growth of the $Gd(OH)_3$ SMRs and Gd_2O_3 SMRs. Base on this point, we adopted different NaOH concentration to study the effect. As depicted in Fig. 4(a), the photoluminescence spectra of Gd_2O_3:18%Yb^{3+},0.5%Tm^{3+} SMRs with different concentration of NaOH show the negative relationship between NaOH content and luminescent intensity, that is, the total luminescent intensities decrease along with the increasing NaOH concentration. From the inset of Fig. 4(a), the morphologies of Gd_2O_3 SMRs hardly change. Under such circumstances, we contribute the phenomenon to the lattice constants which change along with the pH values of the initial reaction solution. As reported by Liu et al. (2014), the lattice constants increase slightly with the increasing pH values, which results into the enhanced NIR emission of the as-prepared $NaYF_4$:Yb^{3+},Tm^{3+} particles. Similarly, the increasing NaOH content will also raise the lattice constants of the precursor $Gd(OH)_3$ and, as a result, raise the lattice constants of Gd_2O_3 SMRs under the same annealing treatment. In this way, the NIR emission will decrease. Therefore, we find that the NIR emission is enhanced by adopting less NaOH concentration in the initial reaction stage.

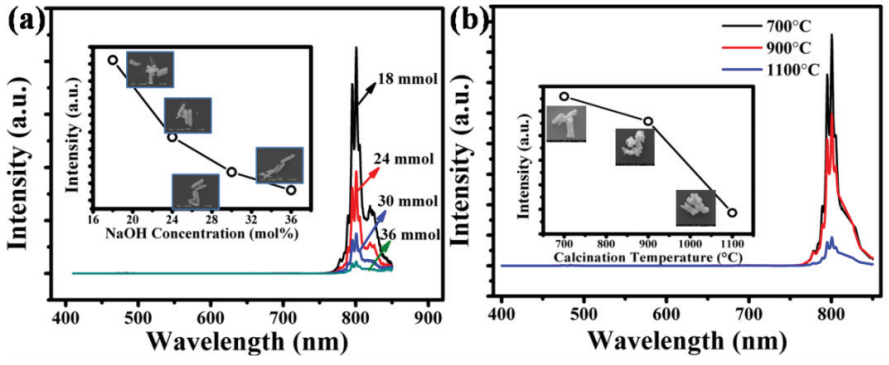

Fig.4 UC emission spectra of Gd_2O_3:18%Yb^{3+},0.5%Tm^{3+} SMRs derived from (a) different alkaline base concentration and (b) different calcination temperatures. Insets show the relationship between the integrated NIR intensities and two factors.

Generally the annealing condition also plays an important role in the luminescence of the rare-earth doped materials. Many researches show that integrated luminescence intensities were positive proportional to the annealing temperatures such as Ningthoujam et al. (2010), Chen et al. (2013) and Hu et al. (2014). However, in our result, this phenomenon is opposite. As depicted in Fig. 4(b), the NIR emission intensity decreases along with the increasing annealing temperature. According to the inset shown in Fig. 4(b), the morphology of SMRs alters with the variation of annealing temperature: with the increase of temperature, the particles gradually form agglomerates. In this situation, there may be two reasons that could lead to the decline of NIR emission. One is that with the agglomeration of particles, the specific area of particles decreases, and thus lowers the concentration of Tm^{3+} ions that distribute around the surface. In this way, the NIR emission could be reduced. The second reason may be that the increasing annealing temperature can distort the lattice space, and due to the difference of ionic radii between Yb^{3+}/Tm^{3+} and Gd^{3+}, the Yb^{3+}/Tm^{3+} ions may probably precipitate out from the crystal, causing the enhancement of local Yb^{3+}/Tm^{3+} concentration. And in this way, the NIR emission could also be lowered due to the quenching effect. However, there is little evidence that support our conjecture, which will be proved in the later experiments.

4. Conclusion

Gd_2O_3 sub-microrods (SMRs) with cubic structure have been obtained via heat-treatment from gadolinium hydroxides precursor, which can be synthesized by a simple hydrothermal route. UC spectra show intense NIR emission which is assigned to Tm^{3+} $^3H_4 \rightarrow {}^3H_6$ transition, and this is the typical two-photon UC process. Moreover, the UC spectra of a series of Gd_2O_3:18%Yb^{3+},x%Tm^{3+} and Gd_2O_3:y%Yb^{3+},0.5%Tm^{3+} SMRs show that 18%Yb^{3+} and 0.5%Tm^{3+} codoped Gd_2O_3 SMRs present the strongest NIR emission. Finally, the enhanced NIR emission property was found in Gd_2O_3:Yb^{3+},Tm^{3+} SMRs from the reduced NaOH concentration and the reduced calcinations temperatures. All the results show excellent NIR emission of our products, suggesting their potential applications in bio-imaging technique.

Acknowledgements

This work was supported by the National Natural Science Foundation of China under Grant No. 61176010 and No. 61172027, the Natural Science Foundation of Guangdong Province of China (Grant No. S2011010001397).

References

Johnson J.C., Choi H.J., Knutsen K.P., Schaller R.D., Yang P.D., Saykally R.J., 2002, Single Gallium Nitride Nanowire Lasers, Nature Materials 1, 106–110

Wang Q.H., Setlur A.A., Lauerhaas J.M., Dai J.Y., Seelig E.W., Chang R.P.H., 1998, A Nanotube-based Field-Emission Flat Panel Display, Applied Physics Letters 72, 2912–2913

Bruchez M., Moronne M., Gin P., Weiss S., Alivisatos A.P., 1998, Semiconductor Nanocrystals as Fluorescent Biological Labels, Science 281, 2013–2016

Law M., Greene L.E., Johnson J.C., Saykally R., Yang P.D., 2005, Nanowire Dye-Sensitized Solar Cell, Nature Materials 4, 455–459

Wang L., Li Y., 2007, Controlled Synthesis and Luminescence of Lanthanide doped $NaYF_4$ Nanocrystals, Chemistry of Materials 19, 727–734

Zhang J., Shade C.M., Chengelis D.A., Petoud S., 2007, A Strategy to Protect and Sensitize Near-Infrared Luminescent Nd^{3+} and Yb^{3+}: Organic Tropolonate Ligands for the Sensitization of Ln^{3+}-Doped $NaYF_4$ Nanocrystals, Journal of the American Chemical Society 129, 14834–14835

Chen G., Ohulchanskyy T. Y., Kumar R., Agren H., Prasad P. N., 2010, Ultrasmall Monodisperse $NaYF_4$:Yb^{3+}/Tm^{3+} Nanocrystals with Enhanced Near-Infrared to Near-Infrared Upconversion Photoluminescence, ACS Nano 4, 3163-3168

Chang J., Liu Y., Li J., Wu S., Niu W., Zhang S., 2013, Strong Red and NIR Emission in $NaYF_4$:Yb^{3+},Tm^{3+}/QDs nanoheterostructures, Journal of Materials Chemistry C 1, 1168-1173

Liu B., Wang J., Zhu L., Zhang H., Chen H., Xu F., Guo K., Zhao J. 2014, Remarkable Enhancement of the Near-Infrared Upconversion Emission in the β-$NaYF_4$:Yb^{3+}/Tm^{3+} system with controllable morphology, Materials Research Bulletin 51, 180-184

Mahalingam V., Vetrone F., Naccache R., Speghini A., Capobianco J.A., 2009, Colloidal Tm^{3+}/Yb^{3+}-Doped $LiYF_4$ Nanocrystals: Multiple Luminescence Spanning the UV to NIR Regions via Low-Energy Excitation, Advanced Materials 21, 4025-4028

Shanta Singh N., Ningthoujam R.S., Dorendraji Singh S., Viswanadh B., Manoj N., Vatsa R.K., 2010, Preparation of highly crystalline blue emitting MVO4:Tm^{3+} (M = Gd, Y) spherical nanoparticles: Effects of activator concentration and annealing temperature on luminescence, lifetime and quantum yield, Journal of Luminescence 130, 2452-2459

Zhu B., Chen N., Zhu D., Li Y., Sun W., Liu G., Du G., 2013, Thermal annealing of LaF_3:Eu^{3+} nanocrystals synthesized by a solvothermal method and their luminescence properties, Journal of Sol-Gel Science and Technology 66, 126-132

Wang Y., Hu X., Zhan S., Sun X., Wang Z., Miao T., Miao H., Fan J., 2014, Annealing temperatures influence luminescence of YBO_3:Ce^{3+},Yb^{3+} prepared by solvothermal method, Journal of Luminescence 152, 188-191